UNIVERSITY OF AMSTERDAM

UvA-DARE (Digital Academic Repository)

Coherent X-ray scattering of charge order dynamics and phase separation in titanates

Shi, B.

Publication date
2017

Document Version
Other version

License
Other

Link to publication

Citation for published version (APA):
Shi, B. (2017). *Coherent X-ray scattering of charge order dynamics and phase separation in titanates*. [Thesis, fully internal, Universiteit van Amsterdam].

General rights
It is not permitted to download or to forward/distribute the text or part of it without the consent of the author(s) and/or copyright holder(s), other than for strictly personal, individual use, unless the work is under an open content license (like Creative Commons).

Disclaimer/Complaints regulations
If you believe that digital publication of certain material infringes any of your rights or (privacy) interests, please let the Library know, stating your reasons. In case of a legitimate complaint, the Library will make the material inaccessible and/or remove it from the website. Please Ask the Library: https://uba.uva.nl/en/contact, or a letter to: Library of the University of Amsterdam, Secretariat, Singel 425, 1012 WP Amsterdam, The Netherlands. You will be contacted as soon as possible.

UvA-DARE is a service provided by the library of the University of Amsterdam (https://dare.uva.nl)

Download date:28 Apr 2025

Chapter 2

3d Transition Metal Oxides

The 3d transition metal oxides are an extremely large and important class of materials. Many of these have useful and often surprising properties such as the high temperature superconducting compounds [1, 2, 4] and the manganite systems that display the colossal magnetoresistance effect (CMR) [5, 6, 14]. More recently, the interfaces between $SrTiO_3$ and $LaAlO_3$, two insulators, have been shown to be metallic, magnetic and even superconducting [7, 8, 26, 9], highlighting the role also played by titanates.

Although these systems have been studied extensively for decades, they still pose many unresolved questions. This is due to the delicate balance between many energy scales in the system, such as the on-site Coulomb interaction, or Hubbard U, single particle electronic bandwidth, crystal field splitting etc. Often in this case, spin, charge, and orbital degree of freedoms are fluctuating and especially get enhanced toward the metal-insulator transition [20, 27, 28]. The concepts central to the physics of these systems will be introduced and discussed in this chapter.

2.1 Colossal magnetoresistant manganites

The richness in behavior of the 3d transition metal oxides is captured in phase diagrams, which chart the material properties as a function of doping and temperature. To set the stage, let us first deal with a relevant example, which also allows us to introduce many important concepts.

In Fig. 2.1 (b), we show the temperature-doping phase diagram of the CMR compound $La_{1-x}Ca_xMnO_3$ [22]. The parent compound $LaMnO_3$ is an insulator at room temperature, in which Mn has valence 3+ with 3d configuration of $t_{2g}^3\ e_g^1$, due to the dominance of the Hund's rule energy lowering over the cubic crystal field. Below the Curie temperature at 140K, the Mn spins are ferromagnetically ordered.

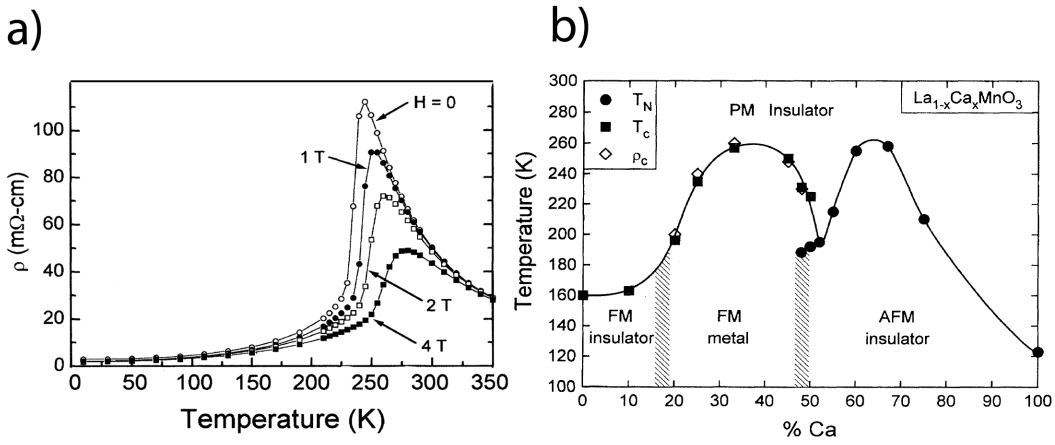

Fig. 2.1 (a) The colossal magnetoresistance effect of $La_{0.75}Ca_{0.25}MnO_3$. (b) The phase diagram of calcium doped manganites. Taken from Schiffer et al. [22].

Replacing La^{3+} by Ca^{2+} transforms part of the Mn^{3+} ions into Mn^{4+}, effectively removing the e_g electron at some sites (hole doping). This opens up a pathway for conductivity, as the correlation effect raised by strong hybridization between e_g and O 2p electrons is reduced [20]. At high enough doping levels, this leads to a transition to a state that is conducting at low temperatures but insulating at higher temperatures, as shown in Fig. 2.1 (a) for x=0.25. This transition is called a Metal-Insulator Transition (MIT), and in this case it is both intimately linked to the magnetic order as a result of double-exchange interactions [29–32] in the material and to the strong interaction between the electron and the lattice [33].

In the manganites, the MIT is strongly influenced by external magnetic fields, as is visible in the example given in Fig. 2.1 (a), and this field dependence was dubbed the Colossal Magnetoresistance (CMR) effect [5, 22]. The size of the effect has led to the hope that it could be used for applications, which requires developing a material that shows the CMR effect at room temperature. Although this quest has been difficult, the research has led to many surprising findings and deep insights into this class of materials.

Metal-insulator transitions have been found in many transition metal oxides, such as magnetite, cuprates, nickelates and titanates. A comprehensive review has been given by Imada, Fujimori and Tokura [20].

2.2 Phase separation scenario

It is argued that the CMR manganites are intrinsically phase separated, where the ferromagnetic metallic phase competes with an insulating phase [34, 14]. In the phase separation

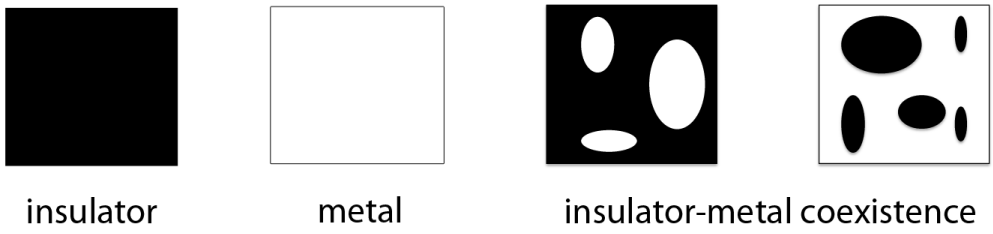

Fig. 2.2 A simple model of 2D phase separation. Left: conventional materials are either an insulator (black), a metal (white), or a semiconductor. Right: in phase separated systems, more than one electronic phase (insulator and metal) coexists. Conductivity is only possible if a percolative metallic pathway (white) connects two edges of the system.

scenario, conductivity takes place via percolative pathways made up of the metallic phase in a matrix of insulating patches (see Fig. 2.2). In the manganites, the CMR effect is then explained by the ability of the external field to align the spins of the ferromagnetic metallic regions, strongly enhancing the conductivity by removing the necessity for spin flips during electron transport through the FM phase [13].

However, it is still being debated whether or not the metal-insulator transitions in complex oxides have a purely electronic origin, since the two electronic phases are also coupled to different types of lattice distortions. In the meantime, a number of pointers from both experiment and theory suggest that structural effects are also playing an important role [21, 34, 15].

Phase separation has been observed in many systems using x-ray diffraction [35–37, 21, 34, 38, 39, 26] or transmission electron microscopy (TEM) [13, 40, 41, 11]. The typical length scale of the phase separation can range from nanometers [40] to microns [41, 13].

The observations suggest that such phase separation is a common scenario in transition metal oxides. In this thesis phase separation will be explored in the titanate family (RCa)TiO_3, where R stands for a rare earth element or yttrium. It will be argued that the titanates studied here show a phase separation phenomenology that in many respects is comparable to that in the manganites, which is surprising in view of the fact that these titanates lack magnetism, and in particular the double-exchange interaction.

2.3 Charge ordering

The phases that play a role in phase separation scenarios also typically involve ordering of charges, orbitals, or spins. In this thesis, our discussion is limited to charge ordering (CO), where the resulting CO structures are mainly due to electrostatic repulsion between charges on transition metal ion sites [42]. Typical examples of charge ordered systems include magnetite [43, 44], and half-doped CMR manganites, where both commensurate and incommensurate charge ordering has been observed [41]. Recently, bulk X-ray scattering data [45–48] have confirmed earlier STM reports [49] that CO also occurs in the cuprate high temperature superconductors.

Very often, the crystal lattice of charge ordered phases is distorted, taking on lower spatial symmetry, for instance from orthorhombic to monoclinic [43, 50, 41, 51]. More importantly, the charge ordered states also produce a superstructure on top of the parent lattice, which can be studied independently using wave vector selective techniques, such as x-ray scattering [45–48].

Recent studies suggest that the charge ordered states compete with superconductivity in the cuprates [46] and with ferromagnetic metallic states in the CMR manganites [52]. An open question is whether these phases are fluctuating at equilibrium and what their dynamics are. Equally, the nature and role of phase separation, also in the titanates [53] is of great interest. These questions form part of the motivation for the work discussed in this thesis.

2.4 Crystal structure of cubic perovskites

In most of the transition metal oxides, the transition metal is surrounded by an octahedral oxygen cage, which forms the standard structural unit of these materials. In between these cages, many other ions can be fitted. We will be dealing here mostly with the cubic perovskites with structural formula ABO_3, where A is an alkaline earth or rare earth ion and B a transition metal ion (Fig. 2.3 (a)). Under the influence of the surrounding oxygen atoms, the 3d shell of the transition metal B ion reorganizes into t_{2g} (d_{xy}, d_{yz}, d_{xz}) and e_g ($d_{x^2-y^2}$, d_{z^2}) groups of levels, where the former group has lower energy.

Depending on the relative sizes of the ions occupying the A and B sites, the MO_6 octahedra can also show a considerable degree of tilting. This leads to what is known as a $GdFeO_3$ distortion and this is shown in Fig. 2.3 (b). Changing the bond angles between the metal ions and the bridging oxygen ions in this manner can strongly influence the ability of electrons to hop between adjacent metal sites. The strength of the induced structural distortion can be expressed in terms of the tolerance factor, which is defined as,

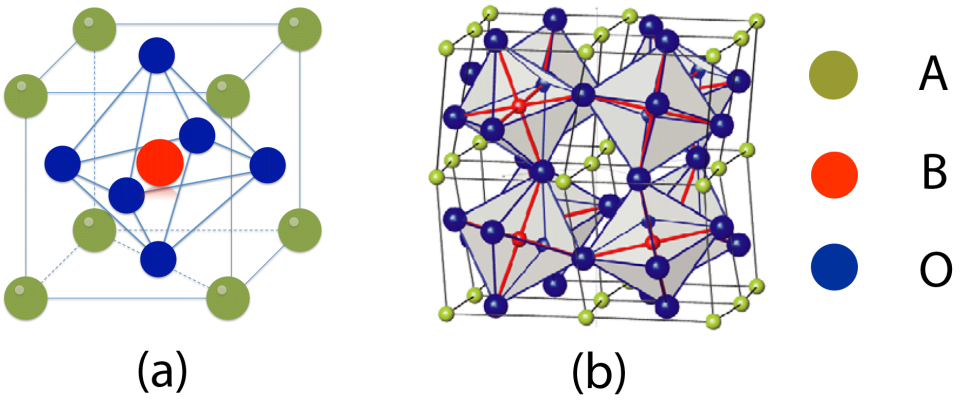

Fig. 2.3 (a) The ideal cubic unit cell for the ABO_3 perovskite compounds. It has the A cation (green) corner shared by 8 neighboring unit cells, and the B cation (red) at the center of an oxygen (blue) octahedron. (b) The crystal structure of the rare-earth titanates $RTiO_3$. Here the octahedral cages that host the titanium ion can tilt and rotate in the same manner as in $GdFeO_3$, hence the name $GdFeO_3$ distortion. In this configuration, even without distortion of each individual oxygen octahedron, the cubic symmetry is broken. The panel (b) is taken from Ref. [54].

$$t = \frac{r_A + r_O}{\sqrt{2}(r_B + r_O)}, \tag{2.1}$$

where the parameters are the radii of A rare earth cation, B transition metal cation, and O the oxygen anion [55, 56]. As we will see these effects can combine to produce changes in the crystal symmetry.

As mentioned previously, in undoped $LaMnO_3$ the four 3d electrons occupy the three t_{2g} orbitals and one of the e_g orbitals. In the undoped titanates that are the subject of this thesis, there is also a single electron in an orbitally degenerate system, but in this case the electron resides in the t_{2g} orbital manifold. The octahedra are easily deformed by preferential occupation of the sublevels of the t_{2g} bands, an effect known as the d-type Jahn-Teller effect [57, 20]. These local Jahn-Teller distortion can also organize in a cooperative manner, further lowering the symmetry of the crystal lattice. Such Jahn-Teller distortions couples the occupancy of particular orbitals with electrons to the lattice degree of freedom [58, 59, 54]. This can even lead to a change in the electron mobility in many different and intricately linked ways.

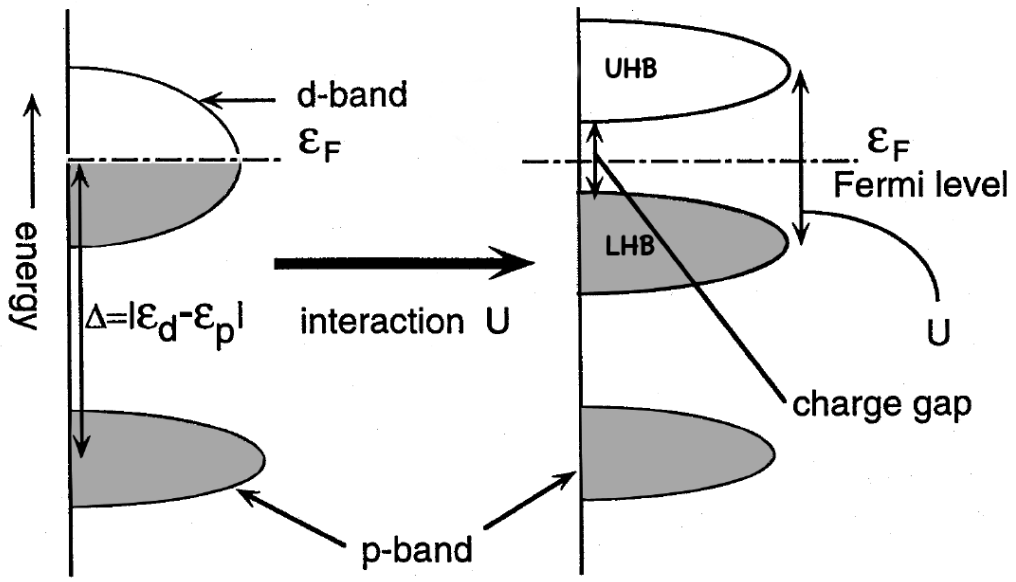

Fig. 2.4 Taken from Ref. [20]. A schematic illustrating the effects of switching on the electron-electron interaction U. The previous metal with half filled d band (left panel) becomes a Mott-Hubbard insulator (right panel) as the U splits the d band into upper Hubbard band (UHB) and lower Hubbard band (LHB) with charge gap, in which the Fermi level lies.

2.5 Electronic structure

In some cases transition metal oxides can be described in terms of standard band theory. Within this framework for the early transition metals, this leads to a filled oxygen *p* band lying under a transition metal 3*d* conduction band (Fig. 2.4 left). Depending on the filling of this band, the systems can be metallic or insulating. However, very often electron correlation effects occur which are a result of the electrostatic repulsion between electrons on the same site. According to the Mott-Hubbard model [60], these effects can lead to a splitting of the 3d band to give what are known as the lower and upper Hubbard band (Fig. 2.4 right).

In dynamical mean-field theory, which is suited for studying materials that are more strongly correlated [61], one can move continuously between the band and Mott-Hubbard models by tuning the parameter U/W, where U is the electron correlation energy and W the width of the conduction band. Starting from a hypothetical uncorrelated metal with a parabolic density of states that is half filled, when the correlation energy is gradually increased, the band deforms accordingly, forming two side lobes around a central peak near the Fermi level. When U/W becomes larger than 1, the central peak disappears and a gap opens up between the lower and upper Hubbard bands.

Thus, correlation effects can transform a metal into an insulator, and we will see that this effect plays an important role in systems with Mott-Hubbard like metal-insulator transitions. Seeing as correlation effects are particularly strong at half-filling, doping strategies can be used to gain control over the electronic behavior. There are two ways to cause an MIT by doping: one can influence the bandwidth W, primarily by influencing the Ti-O-Ti bond angle and thus the hopping parameter (bandwidth controlled MIT). This can be implemented by isovalent substitution at the A site, affecting the octahedral tilting, for example. But also it is possible to change the filling of the band itself, thus manipulating the position of the Fermi level (Fig. 2.4 right), giving rise to what is known as a filling controlled MIT [20]. Here elements are substituted at the A site which have different valency than the A atom has.

2.6 Doping dependence

Before going into a detailed discussion of the MIT in titanates, we will describe first the effects of doping in general. Besides, in some cases, changing the charge carrier concentration, doping can also subtly change the structure, as dopant ions can have different radii than those they replace in the crystal lattice. The A site doping locally alters the tolerance factor, and this can thus be seen as a source of disorder. This can lead to lattice expansion and/or contraction, and the transition metal octahedra can locally tilt to accommodate the dopant ion. Furthermore, doping introduces ionic potential disorder, causing a local break in translational symmetry and via this route, the electronic conductivity is also influenced.

These effects can lead to changes in important local electronic parameters, such as the exchange energies J, hopping parameters t and bandwidth W, but can also set up long ranged strain fields. Very often, all these effects have competing, similar, energy scales which gives rise to these materials' extreme sensitivity to external factors such as pressure, external fields and temperature. It is this interplay that leads to both the richness of the physics and to the intrinsic complexity of these materials.

2.7 The titanates

In comparison to the manganites, titanates had received less attention, due to the absence of the spectacular CMR effect in these compounds. Recently, the $LaAlO_3/SrTiO_3$ and related thin films have been shown to support 2 dimensional electron gases, ferromagnetism and superconductivity, and this has re-kindled the interest in titanates [7]. Nevertheless, for single crystal titanates, apart from the lack of magnetism, there are many important similarities between the titanates and the manganites, and this makes them interesting to study, also

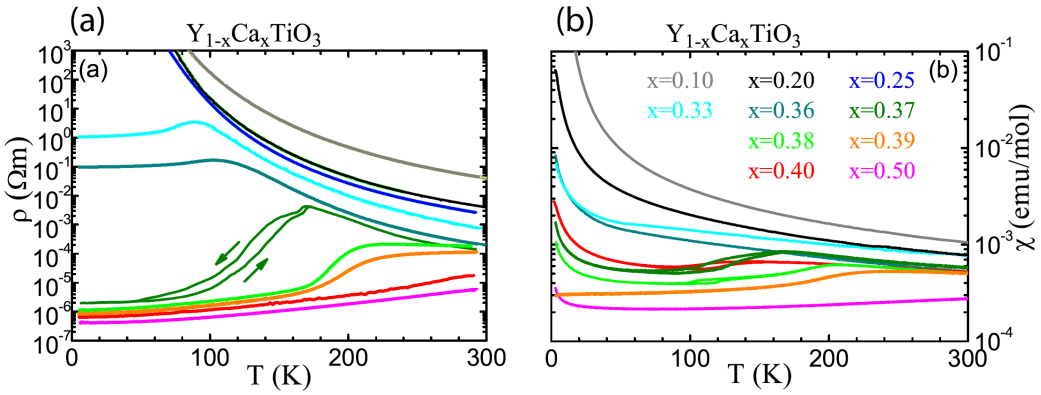

Fig. 2.5 (a)The temperature dependence of the resistivity, (b) the susceptibility of the (YCa)TiO_3 system. Data from A. C. Komarek [16].

as a kind of non-magnetic control experiment for theories developed for the manganites. MITs abound in the titanate system due, in part, to the narrow bands resulting from the $pd\pi$ overlap, which is common in perovskites in which only t_{2g} orbitals are occupied [20].

We will start with a discussion of the (YCa)TiO_3 system, which is one of the best studied series [20, 62, 58, 23, 59]. Experimental data showing the MIT as a function of Ca doping are given in Fig. 2.5. For low Ca-doping the material behaves as an insulator and for high doping as a metal. For intermediate doping values around x=$\sim$ 0.35 the data show a temperature dependent MIT, with strong hysteresis in both the resistivity and the susceptibility.

2.7.1 Filling control in doped titanates

Extensive spectroscopic [63, 62, 19] and theoretical investigations [59, 58] for these type of titanates have led to the following picture (Fig. 2.6), which we first discuss for the (Y,Ca) doping series. In the titanates, U=5 eV, and the bandwidth of $YTiO_3$ is 2 eV [20, 59]. Pure $YTiO_3$ is therefore a Mott-Hubbard insulator possessing also a $GdFeO_3$-type distortion and strong orbital ordering [20, 59, 54]. This order is stabilized by the large tilting of the octahedra by up to 20°, which on the one hand narrows W due to Ti-O-Ti bond angle effect, but on the other hand enhances the covalent overlap between the O 2p states and the Y states via pd-π-type interactions [59]. The tilting splits the threefold degenerate t_{2g} subband, which lowers the $U_{critical}$/W, bringing the system deeper into the Mott insulating phase [27].

Doping $YTiO_3$ with calcium gives a clear example of a band filling induced insulator to metal transition. Y^{3+} and Ca^{2+} ions have the same ionic radius, hence when replacing Y ions by Ca ions, the structure stays roughly constant. As Ca ions bring one electron less to the system as a whole, part of the Ti ions will take on a valence of 4+. Doping with Ca

therefore results in hole doping, bringing the Fermi level into the lower Hubbard band, as is seen from optical spectroscopy and photoemission studies [62, 63].

As a result of the doping, also the orbital order and low temperature ferromagnetism of the parent compound are weakened, as the holes break up the long range coherence of the structure, resulting in a reduction of U/W as witnessed by the appearance of a quasiparticle peak in the Mott-Hubbard gap, as seen by photoemission [63]. For doping levels around x=0.6, the material is a correlated metal while the end member $CaTiO_3$ is a d^0 band insulator, like the better known $SrTiO_3$.

In Fig. 2.6, we illustrate this general behavior for the particular case of the (Er,Ca) doping series, as this material has also been intensively studied in this thesis research. This figure is based upon a compilation of data from the (Y,Ca) system [20, 21], together with recent data from the (Er, Ca) family itself from Komarek [16].

2.7.2 Crystal structure deformation and charge ordering

The structure of Ca doped rare earth titanate system, especially for $(YCa)TiO_3$ and $(ErCa)TiO_3$ has been investigated in some detail using neutron and x-ray scattering [21, 23, 16], also in the doping region where the temperature-dependent metal insulator transition takes place. It was found that in this region the (011) and (013) diffraction peaks, which are symmetry forbidden in both the cubic and orthorhombic structures, are present [21, 23, 16]. This has been interpreted in terms of further symmetry lowing of the structure due to checkerboard charge order, and Fig 2.7 shows how the CO leads to new sets of equivalent lattice plane giving rise to these formerly forbidden reflections. The neutron studies [23] show that the forbidden reflections still possess intensity below the MIT transition temperature, where transport shows the system to be a metal. The x-ray diffraction studies [16] show CO peak intensity only around the MIT transition itself. These apparently contradictory findings can be reconciled by noting that neutrons primarily are sensitive to atomic (nuclear) positions, while x-rays are sensitive to the electron density per site. This point will be returned to later in chapter 4.

The scattering studies [21, 16] also made it clear that around the MIT, two phases coexist (see Fig. 2.6). The insulating, high temperature orthorhombic (HTO) phase transforms into a mixture of a low temperature monoclinic (LTM) phase and a new, low temperature orthorhombic (LTO) phase with a smaller unit cell compared to the LTM structure [21, 16]. The charge order seen in the neutron scattering was suggested to exist in the LTM phase. The charge ordered LTM unit cell structure is indicated in blue in Fig. 2.7, and is indicated in Fig. 2.6 by the gray shaded regions.

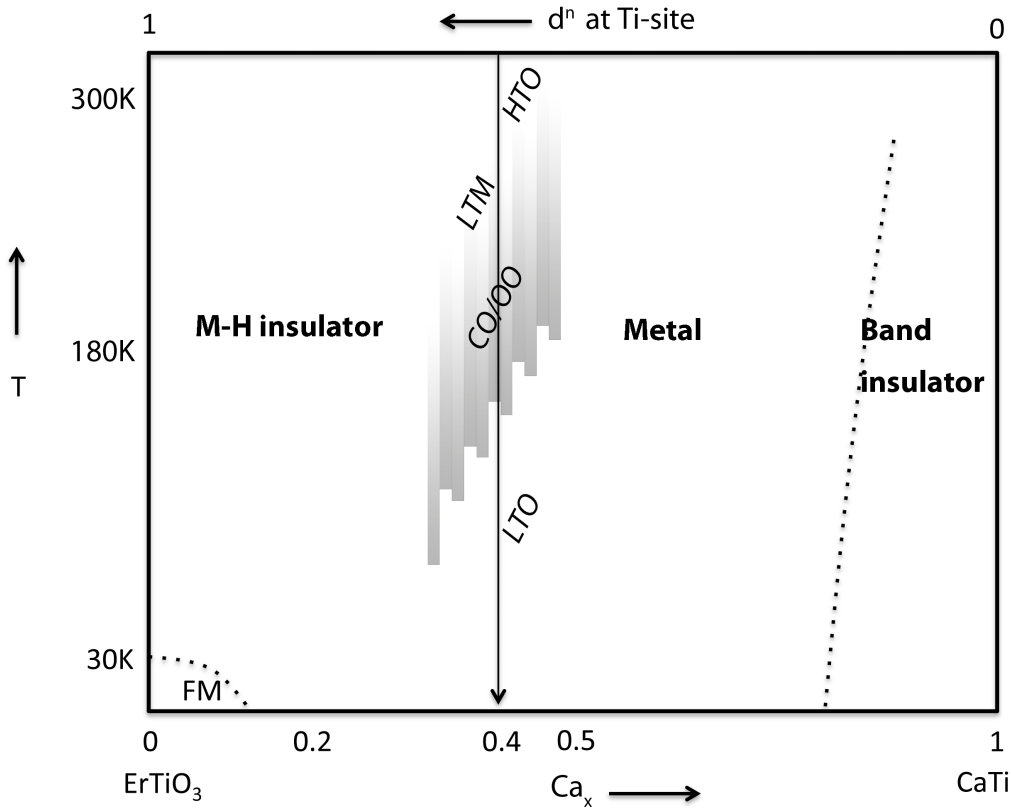

Fig. 2.6 Approximate temperature-doping phase diagram for the system (ErCa)TiO_3, concentrating on the region around the MIT centered at $Er_{0.6}Ca_{0.4}TiO_3$. The parent compound $ErTiO_3$ is a Mott-Hubbard insulator with low temperature ferromagnetism, which disappears rapidly on hole doping. For Ca dopings around 0.4, which means 0.6 3d electrons per Ti site on average, the system displays an insulator to metal transition on cooling, which is accompanied by phase separation and charge ordering. The gray regions sketched around x=0.4 illustrate schematically the CO development during cooling, whereby a darker shade of gray corresponds to a higher degree of CO. On further hole doping, the system develops into a metal, before further emptying of the 3d states eventually turns the system into a band insulator.

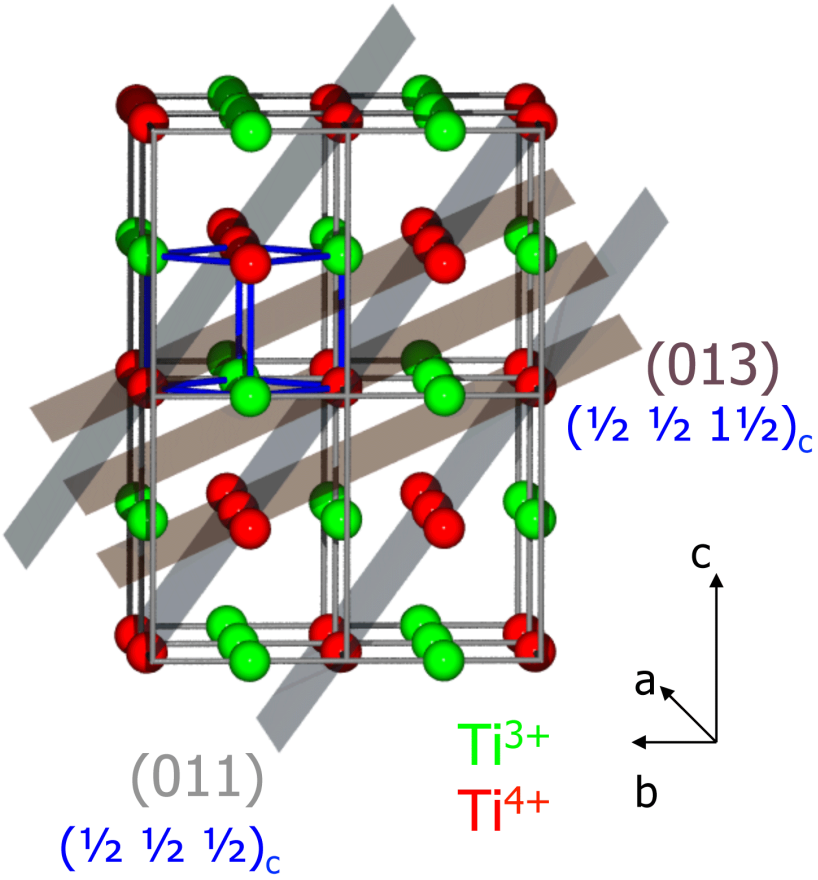

Fig. 2.7 A schematic 3D model of the charge ordered structure of $Y_{0.5}Ca_{0.5}TiO_3$. Red and green balls indicate Ti^{4+} and Ti^{3+} sites respectively. The blue frame indicates one unit cell of the charge-ordered, low temperature monoclinic structure. The shaded bands indicate the charge-ordered (011) and (013) lattice planes. The indexing of the diffraction planes are given in both orthorhombic (grey), and cubic notation, with the latter labeled in blue with a subscript 'c'.

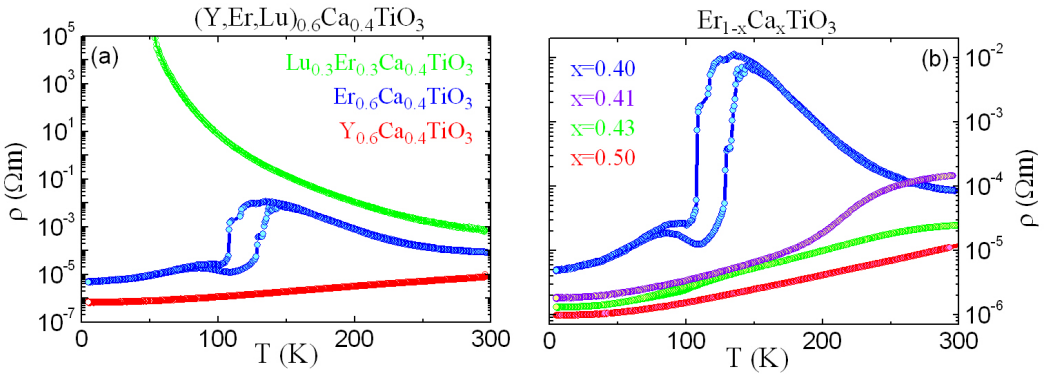

Fig. 2.8 Transport measurements of $R_{1-x}Ca_xTiO_3$. The left graph plots the temperature dependent resistivity measurements for different R cations (Y, Er,Lu), for which the ionic radius decreases along this series. The data in the left panel show a tilting tuned metal insulator transition. On the right side, the graph shows explicitly the doping tuned metal insulator transition with fixed R ion (Er). The metal-insulator transition exhibits a thermal hysteresis. Data from Ref. [23].

2.7.3 Bandwidth control in doped titanates

Komarek et al. [23] have shown that the MIT can also be induced at fixed carrier concentration by replacing the Y ions with rare earth ions of smaller radius. In Fig. 2.8 (a), this is illustrated for a series of $R_{0.6}Ca_{0.4}TiO_3$ compounds, where the R ions, Y, Er and Lu have successively smaller radii. Here the MIT is purely the result of bandwidth control: the smaller R ions cause a strong increase of the tilting of the octahedra, leading to a reduction of W and a transition into the Mott insulating state. Since $Er_{0.6}Ca_{0.4}TiO_3$ was found to have a very strong charge order reflection in X-ray scattering and because it shows the hysteretic transport behavior at its MIT indicative of phase separation, this particular compound was selected for most of the work presented in this thesis. Fig. 2.8 (b) shows a number of resistivity curves showing that the insulator to metal transition for (ErCa)TiO_3 occurs at slightly higher hole doping levels than in the (YCa)TiO_3 system due to the tilting induced reduction of the bandwidth of the (ErCa)TiO_3 system.

The situation can be summarized using a phase diagram as shown in Fig. 2.9, where the different doping series are shown in the U/W versus doping plane, which is based on a similar figure in Ref. [63]. Different electronic phases are indicated in colors. The region in which a transition between MHI and metallic behavior can be realized by cooling from room temperature is indicated as a shaded band sandwiched between the MHI and metallic phases. The blue slanting line indicates the behavior of the (LaSr)TiO_3 system, included as a reference. La is bigger than Y, and as a result the Ti-O-Ti bonds are much less tilted

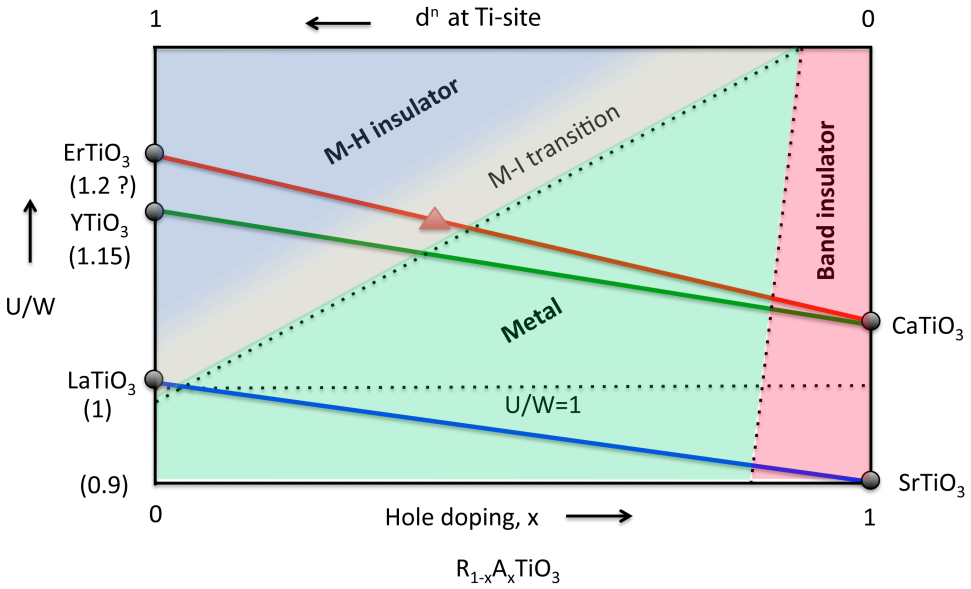

Fig. 2.9 Phase diagram of doped rare-earth titanates in the U/W versus doping plane for hole doping level x between 0 and 1 at T=0 K. The corresponding electron count n is indicated at the top. The full lines indicate from bottom to top the evolution of the $(LaSr)TiO_3$, $(YCa)TiO_3$ and $(ErCa)TiO_3$ systems. The red triangle on the red line indicates the position of $Er_{0.6}Ca_{0.4}TiO_3$. The dotted lines give approximate boundaries between the phases indicated by the colored regions. Based on [63].

(12°) than those of $YTiO_3$, favoring hopping and increasing the bandwidth, resulting in a U/W of $\sim$1 for doping around x=0.05. Thus, although $LaTiO_3$ is a Mott-Hubbard insulator, a tiny amount of doping with Sr^{2+} ions is enough to bring about a transition to metallic phase [20, 63, 19].

The central sloping green line represents the $(YCa)TiO_3$ system [62, 21]. The sloping red line is for the $(ErCa)TiO_3$ case. The greater slope of this line follows from the slightly greater Ca doping level required to reach metallic behavior compared to Ca doping $YTiO_3$, as described above.

In this chapter, the basic properties and characteristics of transition metal oxides in general and of the family of doped titanates which are the subject of the experimental investigations have been reviewed. Without attempting to give an exhaustive account, central concepts such as single-particle bandwidths, Coulomb repulsion, charge order and $GdFeO_3$-type distortions have been mentioned, and their interplay is seen to give rise to a complex phase diagram for Ca-doped $RTiO_3$ (R=Y, Er). Importantly, these systems show a clear, ambient pressure metal to insulator transition in an experimentally accessible temperature range. This MIT resembles that of much-studied transition metal oxide systems such as the manganites, and it is sensitive to both Ca doping level and R-site ionic radius. In addition it exhibits phase separation phenomena, and clear hysteretic signature in transport and susceptibility, indicating a first order phase transition.

On a general level, a first order phase transition involves the dynamics of both the nucleation and growth of domains. In Chapter 4, the results of experiments using x-ray correlation techniques are reported that are of relevance to aspects of the temperature-driven dynamics of charge order in the MIT of the titanates. In addition, data from different experiments are presented that are designed to hunt for equilibrium dynamics of the charge ordered patterns in such systems (i.e. when the sample is held at constant temperature).